6th International Meeting
on
Wind Turbine Noise
Glasgow, 20-23 April 2015

Low Frequency Acoustic Near Field Of Wind Turbines

Werner Richarz, 76 Roxborough Ln., Thornhill, ON, L4J 4T4 Canada.
wricharz@gmail.com

Summary
The virtual source model of Gutin has been used to determine the unsteady pressure field near a wind turbine. The analysis explicitly identifies the relative contributions of the so-called acoustic near-field to the overall sound levels at the blade passage frequency and low order harmonics. The results show that under certain circumstances the acoustic near-field supplants the propagating sound field. However, this diminishes rapidly with distance from the wind turbine.

Introduction
A good deal of analysis of wind turbine sound is based on sound power estimates determined from measurements at 100m from the wind turbine. While this is sufficient for audible sound, this may not hold true for very low frequency signals such as the blade passage frequency and the first few harmonics. The rotor blades of modern large wind turbines rotate rather slowly, generating blade passage frequencies (BPF) at or below 1Hz. As can be seen from the table below, the associated wavelength of the blade passage frequency is substantial.

RPM	6	8	10	12	14	16	18	19
BPF (Hz)	0.30	0.40	0.50	0.60	0.70	0.80	0.90	0.95
λ (m)	1133	850	680	567	486	425	378	358

Virtually all acoustic sources have a near-field where unsteady perturbations that are not associated with the net transport of acoustic energy have magnitudes greater than or comparable to the 'propagating' acoustic field. These disturbances typically diminish in inverse proportion to the square of the source-receiver distance $1/SRD^2$; acoustic perturbations decay as $1/SRD$.

The concern about adverse effects has fueled much speculation about the ultra-low frequency tones emitted by wind turbines. Accurate measurement of the sound pressure level of the blade passage frequency and the first few harmonics requires specialized instrumentation as well as favourable atmospheric conditions. In order to obtain good signal to noise ratios, it is necessary to minimize the source-receiver distance. For audible sound 100m from the base of the tower has become the norm. At

this distance the acoustic near field of the blade passage frequency may be dominant. The analysis described below explores the relative contributions of the acoustic near and far fields.

Only a few researchers have access to computational acoustic software that may be capable of solving the sound emission from a wind turbine. In principle, the approach taken by Gutin [1] to model the periodic sound emitted from a propeller should also apply to wind turbines. The methodology is sufficiently accurate (for subsonic tip speeds) if the blade loading is described with reasonable accuracy. Morse and Ingard [2] have given a more analytic perspective and addressed the case of non-uniform inflow. No attention was paid to the acoustics near field.

Garrick and Watkins [3] extended Gutin's method to include rectilinear translation of either the source or the observer. Their principal motivation was to understand the effect of forward speed on the sound field of a propeller. The near field was also important as it impacted the interior noise of commercial transports were then all propeller driven. The derivations and discussions in reference [3] quite detailed yet without much un-necessary mathematics. Of special interest is the retention of the acoustic near field, which will be examined for rotors of wind turbines.

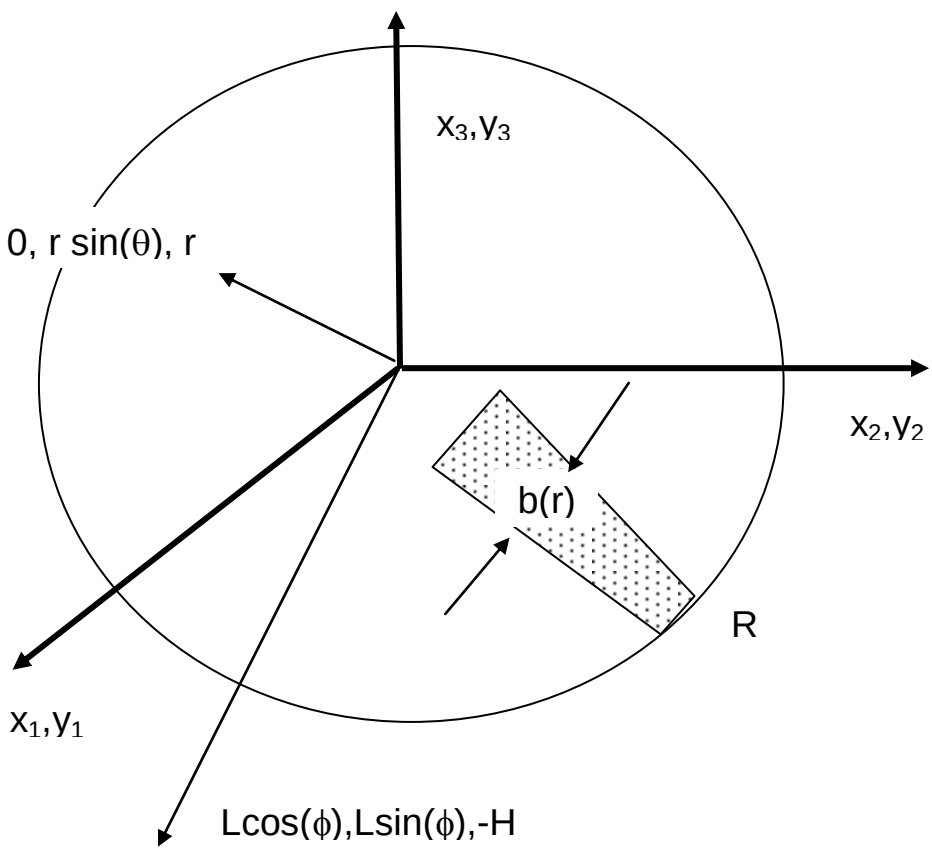

Figure 1. Source and field point co-ordinates,
ϕ is the azimuth angle, $R = 50$m, $H = 100$m,

Underlying Physics

The schematic in figure 1 illustrates the principal co-ordinates and parameters used herein. The analysis is restricted to uniform loading, although could be extended to address unsteady loading due to wind-shear, if sufficiently accurate temporal blade loads are available.

Lamb [4] shows that a force $\boldsymbol{F}$ at $\boldsymbol{y} = (y_1, y_2, y_3)$ induces a pressure at $\boldsymbol{x} = (x_1, x, x_3)$:

$$p(\boldsymbol{x}, t) = \frac{1}{4\pi}\nabla.[\frac{\boldsymbol{F}\left(t - \frac{s}{c}\right)}{\boldsymbol{s}}] = \frac{1}{4\pi}\left\{\frac{\partial}{\partial x_1}\frac{F_1(t - s/c)}{s} + \frac{\partial}{\partial x_2}\frac{F_2(t - s/c)}{s} + \frac{\partial}{\partial x_3}\frac{F_3(t - s/c)}{s}\right\}$$

$$s = \sqrt{(x_1 - y_1)^2 + (x_1 - y_1)^2 + (x_1 - y_1)^2}$$

Upon differentiating the expression the pressure written as $p_{NF}(x, t) + p_{FF}(x, t)$ to show the near field and far-field terms:

$$p_{NF}(x, t) = \frac{1}{4\pi}\frac{-1}{s^2}\{\frac{x_1 - y_1}{s}F_1(t - s/c) + \frac{x_2 - y_2}{s}F_2(t - s/c) + \frac{x_3 - y_3}{s}F_3(t - s/c)\}$$

$$p_{FF}(x, t) = \frac{1}{4\pi c}\frac{-1}{s}\left\{\frac{x_1 - y_1}{s}\frac{\partial F_1(t - s/c)}{\partial t} + \frac{x_2 - y_2}{s}\frac{\partial F_2(t - s/c)}{\partial t} + \frac{x_3 - y_3}{s}\frac{\partial F_3(t - s/c)}{\partial t}\right\}$$

Note that both disturbances propagate at the speed of sound (c). The popular notion that the acoustic near field is associated with an incompressible field is not valid. It is also apparent that if $|\boldsymbol{x}| \gg |\boldsymbol{y}|$ the far field pressure will dominate and certain simplifications may be introduced. Now for an observer moving with the rotor blade will note that the force thereon is steady. The generation of an audible sound by the motion of an otherwise time-invariant is counterintuitive for some. Reference [5] should be consulted to aid in the resolution of the paradox. The generalization of the above has been described in scientific and technical papers and books, too numerous to mention here.

Generalized Source Distribution

Following Gutin [1], the real sources that move in circular pattern about the rotor axis are replaced with a distribution of stationary sources located on a flat disk in the plane of the rotor blades. These sources are only active when covered by the projection of virtual rotor blade.

As a first approximation the time history of the force at a source point is modelled as a periodic function with fundamental frequency. Within each time frame, $T_1 = 1/B\Omega$, the force is non-zero for an interval τ_1. The idealized force-time history, shown in figure 2, resembles the loading of most wind turbine blades [6]. The signal duration is set by the time the projected blade chord (b) dwells over a source point: it is $b/\Omega r$. The signal will be similar for all sources on the disk. The magnitude and duration are determined by the

blade plan form and the loading thereon. The number of blades and the rotation rate determine the relative phase of the sources.

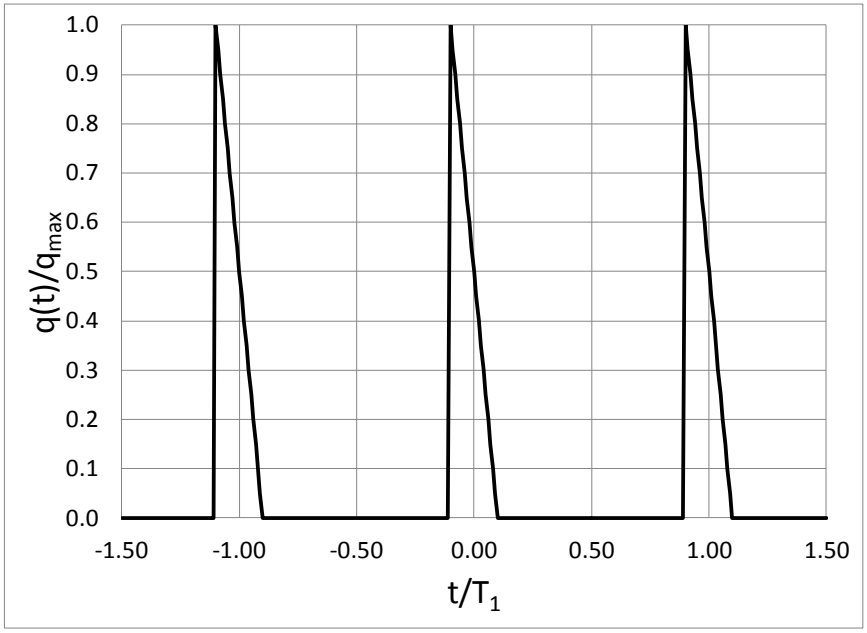

Figure 2. Idealized source function for a three-bladed rotor

The idealized time history is proportional to the blade load. The assumed triangular loading is expressed as the sum of an even and an odd function: $q(t)/q_{max} = 0.5(1 - 2\,t/\tau_1)$, thereby simplifying the Fourier series representation [7]:

$$\frac{q(r,t)}{q_{max}(r)} = \sum a_n \cos\frac{2Z_n t}{\tau_1} + b_n \sin\frac{2Z_n t}{\tau_1}$$

$$a_n = \frac{1}{\pi n}\frac{\sin Z_n}{Z_n},\ b_n = \frac{1}{\pi n}(\cos Z_n - \frac{\sin Z_n}{Z_n}) = \frac{1}{\pi n}\ \ Z_n = \frac{\pi n \tau_1}{T_1}$$

Both T_1 and τ_1 are key parameters. $\tau_1\ /T_1 = B\,b/(2\pi r)$ is the rotor solidity at radius σ_r. Both a_n and b_n are functions of the radial position.

Virtual Propeller Forces

So far the discussion has avoided explicit reference to the rotor forces. The center of the rotor disk is at $(0,0,0)$ and the blades rotate about the x_1 axis. The source co-ordinates are $[0, r\sin\theta\,, r\cos\theta]$, and the field point is at $[L\cos\varphi\,, L\sin\varphi\,, -H]$.

For axisymmetric loading the in-plane forces are $F_2 = D\cos\theta,\ F_3 = -D\sin\theta$. D is a function of radial position and the time history is governed by $q(t)$. The formulation for $q(t)$ does not account for the angular position of the rotor blades. This is easily remedied by replacing t with $(t - \theta/\Omega)$.

The power extracted from the air is proportional to the product of the axial force and the wind speed $(F_1 U)$ as well as the product of the torque and rotation rate $(D\Omega \mathrm{R}^*)$. As a first approximation): $D = F_1\, U/\Omega \mathrm{R}^*$. The force at (r, θ)

$$\boldsymbol{F}(r,\theta,t) = [1, -U/\Omega \mathrm{R}^* \cos\theta\,, U/\Omega \mathrm{R}^* \sin\theta] q(r,t) r dr d\theta$$

induces an acoustic pressure

$$dp = \frac{r dr d\theta}{4\pi s^3}[L\cos\varphi - \frac{U}{\Omega R^*}(L\sin\varphi\cos\theta + H\sin\theta)][q(r, t - \frac{s}{c} - \frac{\theta}{\Omega}) - \frac{s}{c}\frac{\partial q(r, t - \frac{s}{c} - \frac{\theta}{\Omega})}{\partial t}]$$

Summation over the rotor disk is performed numerically. The procedure treats the in-phase $(\cos)$ and quadrature $(\sin)$ contributions separately. This removes any explicit time dependence from the integral. The relative phase of the sources is accounted for by the term. θ is measured with respect to the $y_3$axis. The loading assumes a constant vorticity distribution along the blade, vanishing rapidly near the blade tip. There are no sources near the hub when $r < 0.2R$. The blade has a linearly decreasing (projected) chord.

360 points were used for the integration over θ. It was found that for the assumed loading and blade plan form 30 control points were sufficient. MathCad was used to perform the double summation and the results were exported to a spread sheet for post-processing. Contributions for the near field and far-field pressure are evaluated separately:

$$p_{NF}(n, L, \varphi, t) = A_{NF}(n, L, \varphi, t)\cos(2\pi n f_0 t) + B_{NF}\sin(2\pi n f_0 t).$$

$$p_{FF}(n, L, \varphi, t) = A_{FF}(n, L, \varphi, t)\cos(2\pi n f_0 t) + B_{FF}\sin(2\pi n f_0 t).$$

The individual RMS levels are $< p_{NF} >= 0.5\sqrt{A_{NF}^2 + B_{NF}^2}$ and $< p_{FF} >= 0.5\sqrt{A_{FF}^2 + B_{FF}^2}$ while the overall RMS level is $< p >= 0.5\sqrt{(A_{NF} + A_{FF})^2 + (B_{NF} + B_{FF})^2}$. In order to highlight the influence of the acoustic near field the predicted levels are normalized:

$$SPL_{NF}(n, L, \varphi) = 20\log[< p_{NF}(n, L, \varphi) >/< P_{FF}(n, L, 0)]$$

$$SPL_{FF}(n, L, \varphi) = 20\log[< p_{FF}(n, L, \varphi) >/< P_{FF}(n, L, 0)]$$

$$SPL(n, L, \varphi) = 20\log[< p(n, L, \varphi) >/< P_{FF}(n, L, 0)]$$

Figure 3 shows that for low rotor RPM the acoustic near field contribution to the overall pressure is greater than that of the propagating wave field. This implies that the acoustic power estimated by a single near field measurement would be no more than 6 dB in error. As both signals are pure tones, the relative phase is important. This accounts for the constructive and destructive interference.

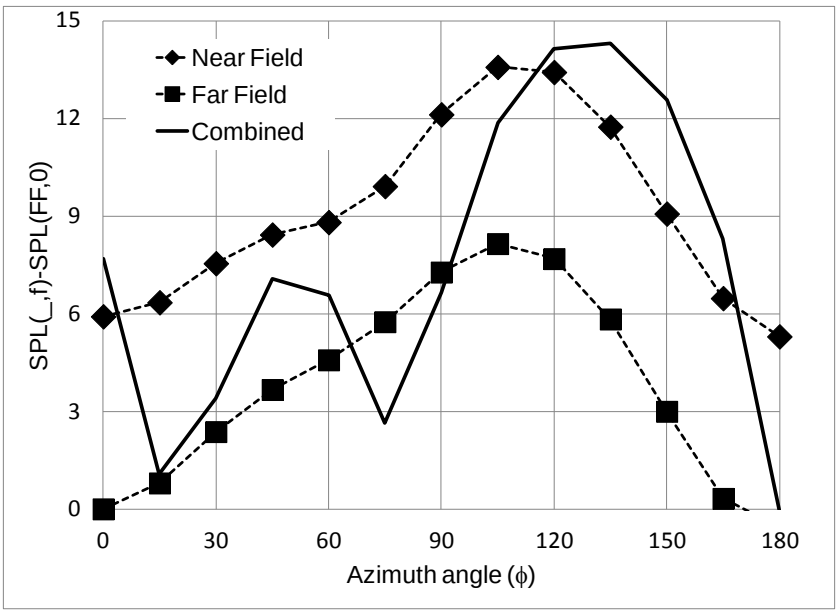

Figure 3. Sound pressures attributed to the acoustic near field of a rotor turning at 8 RPM, field points are 100m from the base of the tower.

For points of observation further out, the relative strength of the near field diminishes. The interference is no longer important and the far-field directivity pattern is approached. The difference between the overall sound pressure level and that of the far field is plotted in Figure 4. In the true far-field the result should be a straight horizontal line. It is seen that this condition is almost reached at 400 from the tower for the blade passage frequency. The nominal near field extends to 850m.

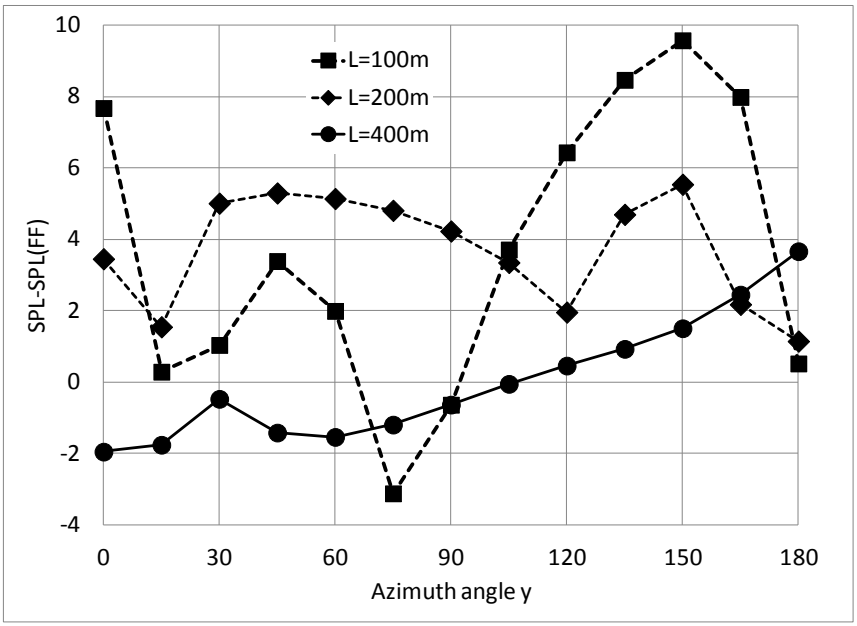

Figure 4. Difference in overall sound pressure level and SPL of far-field portion, RPM=8.

When averaged over all azimuth angles, the effective decay rate of the near-field is 6dB higher than that for the far-field (Figure 5).

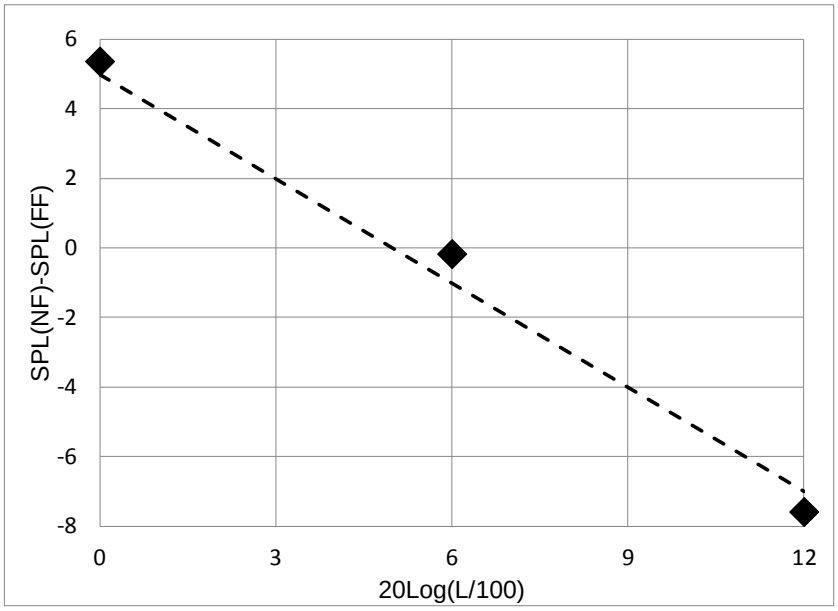

Figure 5. Comparison of decay rates of the sound pressure levels of near field and far field sound. Rotor RPM=8.

As the frequency of the signal increases, either in terms of the harmonic index n or the rotor RPM, the acoustic near field retreats towards the rotor disk. Figure 6 shows the trend for increased rotor RPM.

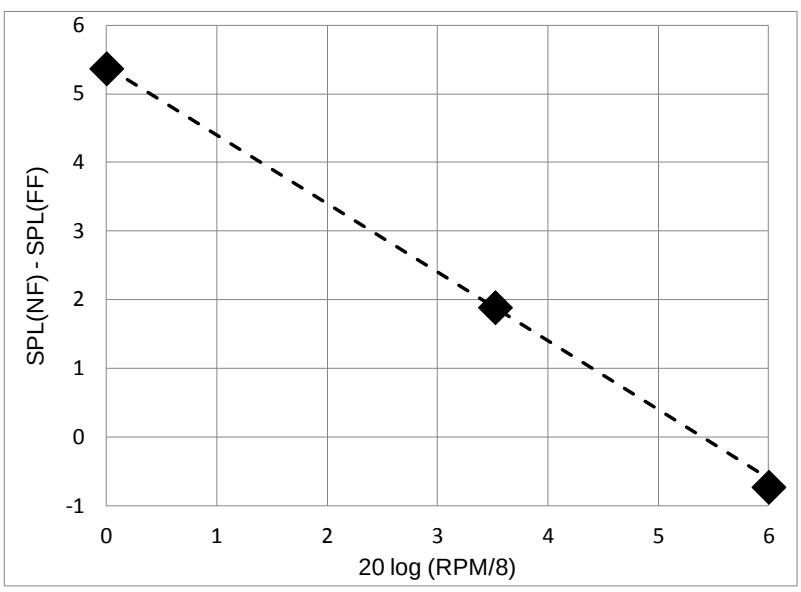

Figure 6. Relative strength of the acoustic near field as a function of rotational speed. Data is averaged over $\varphi = 0_o$ to 180°, L=100m.

Rotor wake - tower interaction

The formalism has been extended to examine the sound associated with interaction of the rotor wake with the tower that supports the wind turbine hub and generator assembly. Acoustic imaging [8] suggests that the interaction is not a significant contributor to audible sound. Dooley and Metelka [9] have suggested a spinning modes does generate a substantial low frequency sound at the blade passage frequency and its harmonics.

As the sound is radiated by the passage of the wake over the tower, the source is only active for brief intervals. The resultant aerodynamic force is almost parallel to the rotor axis so that resultant acoustic pressure is proportional to

$$p_w = \frac{1}{4\pi s^3}[L\cos\varphi][q_W(r, t - \frac{s_w}{c} - \frac{\pi}{\Omega}) - \frac{s_w}{c}\frac{\partial q_w(r, t - \frac{s_w}{c} - \frac{\pi}{\Omega})}{\partial t}]$$

the subscript denoting wake-tower interaction. The idealized source distribution is shown in figure 7.

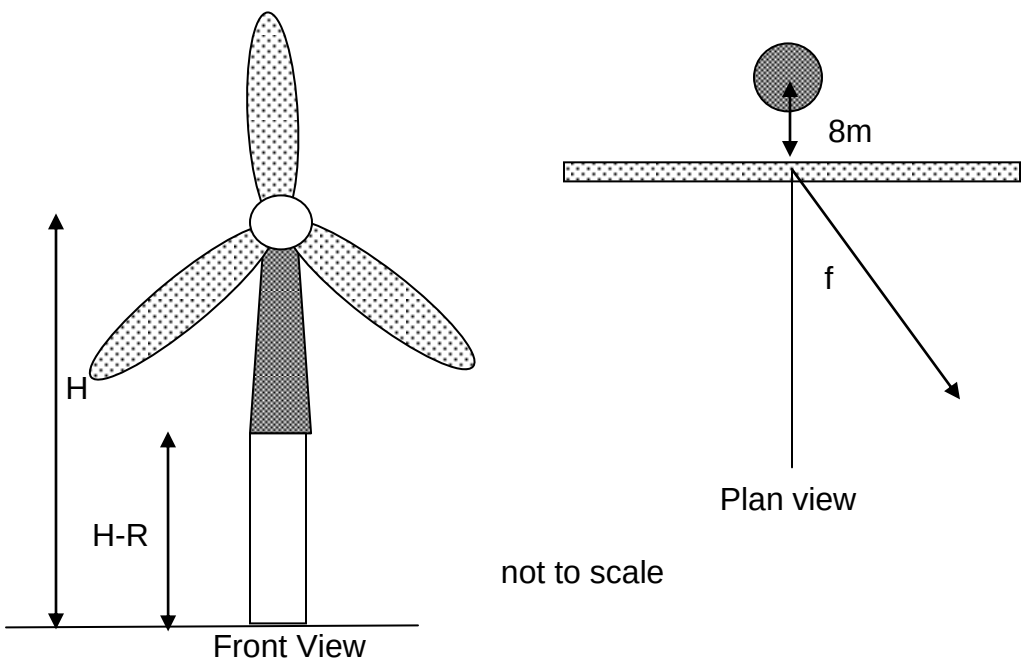

Figure 7. Sources in wake-tower interaction model; source areas are shaded.

The loading function is similar to the one used for the rotor disk. The roll up of the tip vortices may induce larger loads in the outer portion of the wake. The enormous mismatch of the physical dimensions of the scattering surfaces and the acoustic wavelength do not support the resonance model described in reference 9. It is more likely that the signals will be forward scattered [10]. Neither effect is incorporated in the model.

The actual loading of the tower is a matter of conjecture. However, it is only possible to establish a trend line that is a function of the unsteady loads on the tower. This is expressed in terms of a 'load transfer function' (LTF). The loading is identical to the one

applied for the thrust loads. Level differences with respect to the 'no tower' base-line are shown in Figure 8.

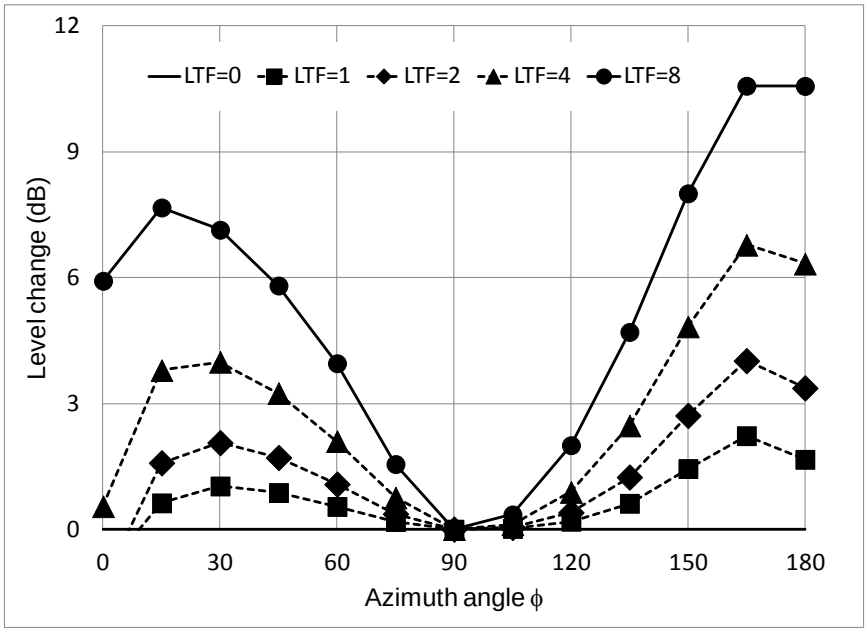

Figure 8. Level changes due to wake-tower interaction, RPM=8, L=100m

The phase difference between the signals from the rotor and the tower vary somewhat with the azimuth angle. Nevertheless the characteristic dipole directivity emerges as the tower loading increases.

Let A denote the overall level of the blade passage frequency from the rotor only. The contribution from the wake-tower interaction is $LTF.W$. For the maximum level change phase effects should be small, so that the level change $\Delta L_{max} \sim 20\log(1 + LTF\frac{B}{A})$. This fits the data surprisingly well for $B/A = 0.3$.

Concluding Remarks

The low frequency pressure field of a modern three bladed wind turbine has been estimated using the virtual source methodology of Gutin and others. Given the low tip Mach number of the rotor blades the formalism is valid. Accuracy is limited only by the degree of similitude of the loading to the ones acting on the rotor blade.

The acoustic near field does make a measurable impact on low frequency sound measured within about 200m from a wind turbine. The predicted changes in sound pressure level are of the order of the measurement accuracy. The predictions of wake-tower interaction are rather tentative and await more accurate load distributions than those used here.

References

1. Gutin, L. — *On The Sound Field Of A Rotating Propeller*, NACA Tech. Memorandum 1195, 1948. Translation of Über das Schallfeld einer rotierenden Luftschraube, Phys. Zeitschrift der Sowjetunion, 9, 1, 1935.

2. Morse, P. M., Ungard, K.U. — *Theoretical Acoustics*, McGraw Hill, pp. 738..747, 1968.

3. Garrick, L.E., Watkins, C.E. — *A Theoretical Study Of The Effect Of Forward Speed On The Free-Space Sound-Pressure Field Around Propellers*, NACA Tech. Note 3018, 1953.

4. Lamb, H. — *Hydrodynamics*, 6th ed., p. 502, Cambridge University Press, 1975.

5. Crighton, D.G., Dowling, A.P., Ffowcs Williams, J.E., Heckl, M, Leppington, F.G — *Modern Methods In Analytical Acoustics*, Springer Verlag, 1992.

6. Burton, T., Jenkins, N., Sharpe, D., Bossanyi, E. — *Wind Energy Handbook*, 2nd ed. Wiley, pp. 66..120, 2011.

7. Duff, G.F.D, Naylor, D. — *Differential Equations of Applied Mathematics*, John Wiley & Sons, pp. 87..94, 1966.

8. Scheppers, J.G., Oerlemans, S — *Sirocco: Silent Rotors by acoustic Optimization*, 2nd International Mtg. On Wind turbine Noise, Lyon, 2007.

9. Dooley, K.A., Metelka, A — Acoustic interaction as a primary cause of infrasonic spinning mode generation and propagation from wind turbines

10. Morse,P.M. — *Vibration and Sound*, pp 347..350, Acoustical Society of America 1976